ELSEVIER

Journal of Organometallic Chemistry 636 (2001) 17–25

Journal of Organometallic Chemistry

www.elsevier.com/locate/jorganchem

Electronic and steric properties of stable silylene ligands in metal(0) carbonyl complexes

Thomas A. Schmedake [a], Michael Haaf [b], Bryan J. Paradise [a], Anthony J. Millevolte [c], Douglas R. Powell [a], Robert West [a,*]

[a] *Department of Chemistry, Organosilicon Research Center, University of Wisconsin-Madison, Madison, WI 53706, USA*
[b] *Elizabethtown College, Elizabethtown, PA 17022, USA*
[c] *University of Wisconsin-Barron County, Rice Lake, WI 54868, USA*

Received 12 February 2001; accepted 27 February 2001

Abstract

A series of stable silylene–transition metal complexes have been synthesized by substitution of silylenes **1** and **2** for carbonyl ligands in simple metal carbonyl complexes: $M(\mathbf{1})_2(CO)_4$ and $M(\mathbf{2})_2(CO)_4$ (M = Cr, Mo, W), $Fe(\mathbf{1})(CO)_4$ and $Ru(\mathbf{1})_2(CO)_3$. X-ray crystal structures are reported. Infrared and NMR spectroscopy were used to probe the electronic properties of stable silylene ligands. Based on these data, the stable silylene **1** behaves electronically very much like triaryl phosphines.

Keywords: Silylene; Coordination complexes; Crystal structure

1. Introduction

Due to their probable intermediacy in several important reactions in organosilicon chemistry, transition metal–silylene complexes have been the subject of considerable interest [1]. A broad assortment of such complexes has now been synthesized with a rich variety of substitution patterns on both the metal and on silicon.

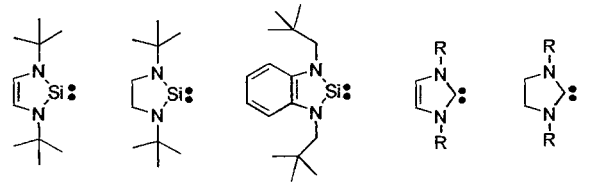

1 **2** **3** **4** **5**

These complexes are characteristically extremely electrophilic, and in this respect are comparable to Fischer carbene complexes [2]. In principle, metal–silylene bonds can be drawn as double bonds (Fig. 1a), though the degree to which π back-bonding occurs from the metal center to the empty p-orbital on the silicon depends profoundly on the attachments to silicon and on the presence of donating solvents. The majority of metal–silylene complexes synthesized so far have required donor stabilization via the addition of a Lewis base [3]. Such complexes exhibit structural and spectroscopic properties that are more similar to metal–silyl complexes than to bona fide metal–silylene complexes and thus, a drawing containing an sp^3 hybridized silicon center (as in Fig. 1b) may be a more appropriate representation [4]. Tilley and co-workers have accomplished the syntheses of several donor-free metal–silylene complexes by utilizing an electron-rich metal fragment and/or by incorporating π-stabilizing substituents (such as thiolates or alkoxy groups) on the electron deficient sp^2-silylene ligand [5]. A sample structure is shown in Fig. 2. The metal–silicon bond lengths in all known silylene complexes are reported to be shorter than a typical M–Si single bond, which may indicate that some degree of multiple bonding is taking place, regardless of the presence of any stabilizing bases.

* Corresponding author. Tel.: +1-608-2621873; fax: +1-608-2626143.
E-mail address: west@chem.wisc.edu (R. West).

0022-328X/01/$ - see front matter
PII: S0022-328X(01)00765-3

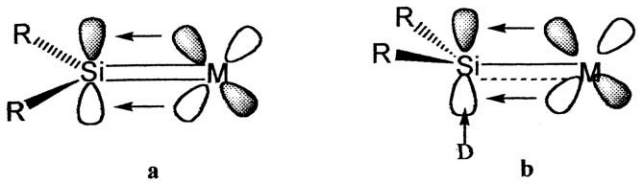

Fig. 1. Schematic drawing of transient silylene ligands on metals: (a) a typical metal–silylene complex; (b) a base-stabilized metal-complex.

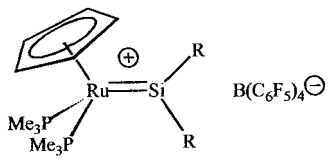

Fig. 2. Base-free metal–silylene complexes (R = thiolate ligand, Me, Ph).

Like the π-stabilized (heteroatom substituted) silylene ligands, N-heterocyclic stable silylenes **1**–**3** benefit from significant donation from the adjacent nitrogens into the empty p-orbital on the silicon [6]. This results in remarkably lowered electrophilicity for the stable silylenes. In fact, they behave primarily as Lewis bases [7]. Consequently, stable silylenes can form stable base-free complexes with transition metals with little back-bonding from the metal to the silicon (Fig. 3). Known complexes of this type include $Ni(\mathbf{1})_2(CO)_2$ [7], $Fe(\mathbf{1})(CO)_4$ [8], $Ni(\mathbf{3})_3PPh_3$ [9], and the homoleptic complexes $Ni(\mathbf{1})_3$ [10], $Ni(\mathbf{2})_3$ and $Pt(\mathbf{3})_4$ [9].

Stable N-heterocyclic carbenes **4** and **5** represent an important new class of organometallic ligands, with electronic properties similar to those of some phosphines [11]. These carbenes have been employed in place of phosphines in transition metal catalysts for reactions such as olefin metathesis and carbon–carbon bond forming reactions, in some cases providing superior catalysis [12]. Complexes of the stable silylenes **1**, **2**, and **3** may also be useful in this manner, but current knowledge of silylene–metal complexes is limited and their effectiveness as ligands in metal catalysts has not yet been established [7,9,13].

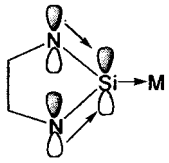

Fig. 3. Schematic drawing of a stable silylene complexed to a metal.

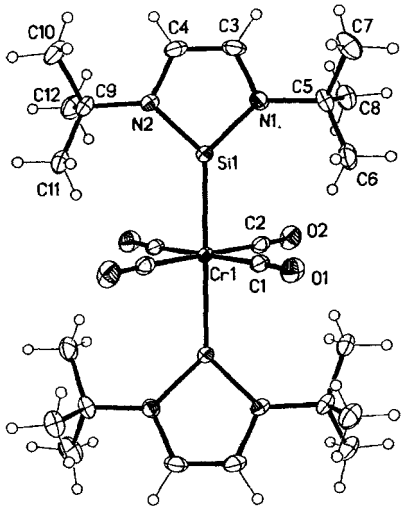

Fig. 4. Thermal ellipsoid diagram for **6**. Structures for **8** and **10** are similar. Relevant bond lengths are summarized in Table 2.

2. Results and discussion

The Group 6 transition metal complexes **6**–**11** were synthesized from the corresponding chromium, molybdenum and tungsten hexacarbonyls and silylene **1** or **2** under photolytic conditions to generate novel complexes with the generic formula *trans*-$M(CO)_4(silylene)_2$ (Eq. (1)).

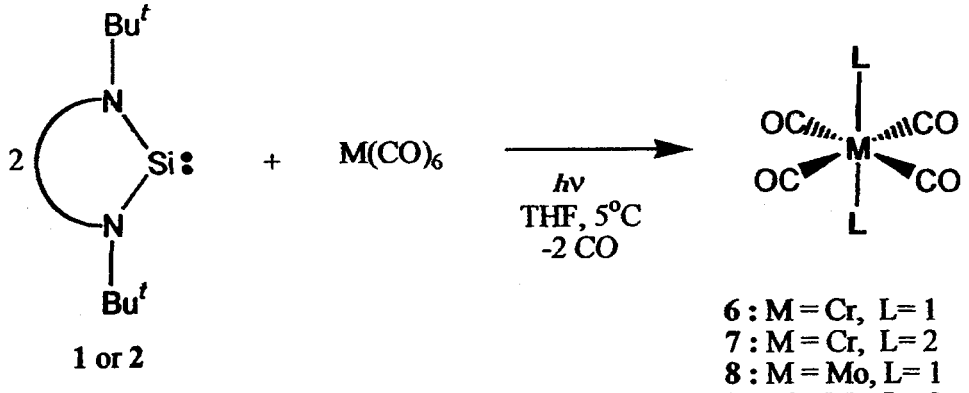

(1)

6: M = Cr, L = 1
7: M = Cr, L = 2
8: M = Mo, L = 1
9: M = Mo, L = 2
10: M = W, L = 1
11: M = W, L = 2

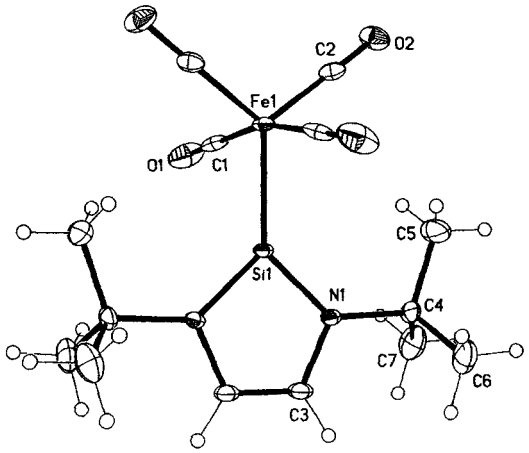

Fig. 5. Crystal structure of **12**. Relevant bond lengths are summarized in Table 2.

4), even when less than two equivalents of silylene is used in the reaction. There is no evidence for the formation of *cis*-substituted octahedral complexes, presumably due to steric constraints. However, NMR evidence indicates the formation of a monosubstituted complex as a minor product in each case.

Two Group 8 complexes were synthesized by mixing silylene **1** with metal carbonyl precursors. As shown in Eq. (2), diiron nonacarbonyl reacted at room temperature with **1** to generate the monosubstituted complex **12** in high yield [8]. Further reaction of the monosubstituted product with excess silylene failed to afford disubstituted product even at elevated temperatures. The structure of this compound was determined crystallographically (Fig. 5).

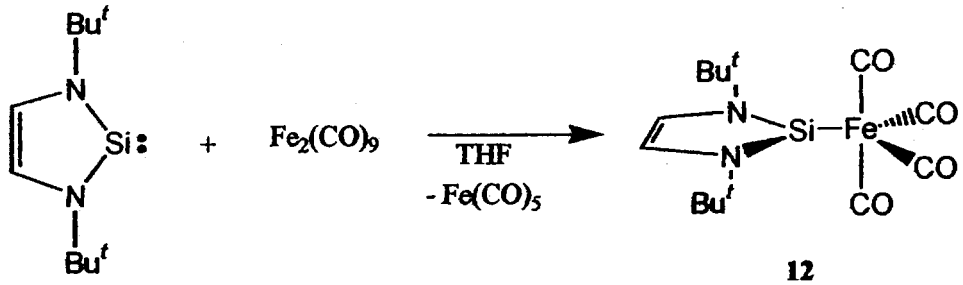

(2)

12

Structures for these complexes were determined crystallographically and a representative example is shown in Fig. 4.

The silylene ligands tend to occupy the least sterically hindered positions about the metal. These d^6-metal complexes preferentially form the *trans*-disubstituted octahedral species (e.g. *trans*-$Cr(\mathbf{1})_2(CO)_4$ shown in Fig.

$Ru(\mathbf{1})_2(CO)_3$, **13**, was synthesized by mixing silylene **1** with $Ru_3(CO)_{12}$ (Eq. (3)). The longer Ru–Si bond (233.0 pm) in comparison to the Fe–Si bond (219.6 pm) is consistent with the fact that the ruthenium center can accommodate two silylene ligands while the iron center has space for only one. X-ray crystallography showed two structures in the asymmetric unit of the unit cell (Fig. 6). Structure A closely approximates a square-pyramidal

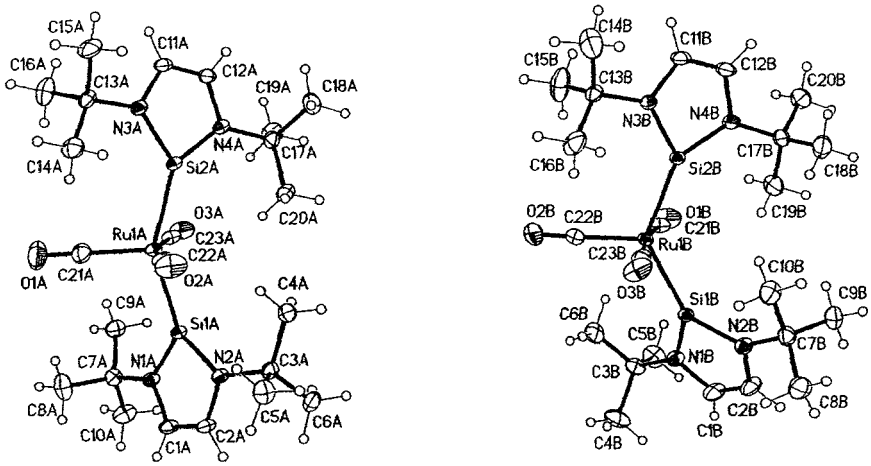

Fig. 6. Crystal structure of **13**. For pertinent bond lengths see Table 3.

Table 1
Comparison of E_u band to similar phosphine compounds

Compound	IR (cm^{-1})	Ref.
$Cr(\mathbf{4})_2(CO)_4$ [a]	1833 E_u	[1]
$Cr[P(Bu)_3]_2(CO)_4$ [b]	1877 E_u	[2]
$\mathbf{9} \sim Cr(\mathbf{2})_2(CO)_4$ [a]	1888 E_u	
$Cr(PPh_3)_2(CO)_4$ [c]	1889 E_u	[3]
$\mathbf{8} \sim Cr(\mathbf{1})_2(CO)_4$ [a]	1889 E_u	
$Cr[P(OMe)_3]_2(CO)_4$ [b]	1912 E_u	[17]
$Cr[P(OPh)_3]_2(CO)_4$ [b]	1930 E_u	[17]
$Mo(\mathbf{4})_2(CO)_4$ [a]	1841 E_u	[16]
$Mo(PMe_3)_2(CO)_4$ [d]	1893 E_u	[4]
$Mo[P(C_2H_5)_3]_2(CO)_4$ [d]	1889 E_u	[18]
$Mo(PPh_3)_2(CO)_4$ [d]	1902 E_u	[18]
$\mathbf{10} \sim Mo(\mathbf{1})_2(CO)_4$ [a]	1904 E_u	
$\mathbf{11} \sim Mo(\mathbf{2})_2(CO)_4$ [a]	1919 E_u	
$Mo[P(OMe)_3]_2(CO)_4$ [b]	1921 E_u	[17]
$Mo[P(OPh)_3]_2(CO)_4$ [b]	1940 E_u	[17]
$W(\mathbf{4})_2(CO)_4$ [a]	1832 E_u	[16]
$W[P(Bu)_3]_2(CO)_4$ [b]	1876 E_u	[17]
$W[P(C_2H_5)_3]_2(CO)_4$ [d]	1880 E_u	[19]
$W(PPh_3)_2(CO)_4$ [e]	1885 E_u	[20]
$\mathbf{12} \sim W(\mathbf{1})_2(CO)_4$ [a]	1896 E_u	
$\mathbf{13} \sim W(\mathbf{2})_2(CO)_4$ [a]	1911 E_u	
$W[P(OMe)_3]_2(CO)_4$ [b]	1916 E_u	[17]
$W[P(OPh)_3]_2(CO)_4$ [b]	1936 E_u	[17]

[a] Benzene.
[b] *n*-Heptane.
[c] CCl_4.
[d] Pentane.
[e] Fluorolube mull.

structure, while structure B is closer to a trigonal bipyramidal arrangement, with the silylene ligands occupying equatorial positions. NMR studies indicate that this complex is isomerizing rapidly on the NMR time scale in solution; the different structures evident in the crystal structure probably result from crystal packing forces. Interestingly, the ^{29}Si-NMR shift of the complex does not change in the presence of the Lewis basic triethylamine, an indication that, like free silylene, the corresponding silylene ligand is not highly π-acidic.

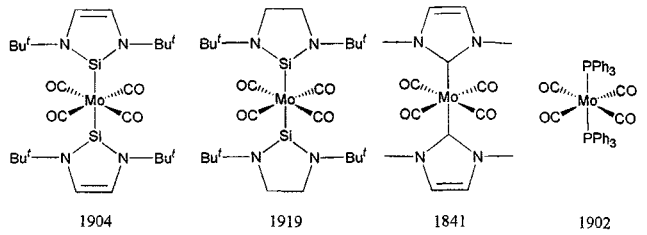

Fig. 7. Some molybdenum complexes and their IR carbonyl stretching frequencies (cm^{-1}).

We used carbonyl stretching frequencies as a probe to compare the electronic properties for a series of ligands. The CO stretching frequencies for the complexes **6, 8,** and **10**, from silylene **1**, are very close to the reported CO stretching frequencies for the series of corresponding compounds with the general formula *trans*-$M(PPh_3)_2(CO)_4$ (see Table 1). A survey of isostructural metal complexes allows for direct comparison of the electronic properties for a variety of common ligands. For example, a molybdenum–carbonyl complex containing N-heterocyclic carbene ligands has significantly lower CO frequencies (1841 cm^{-1}) than the analogous complex with N-heterocyclic silylene ligands (1904 cm^{-1}, see Fig. 7). The same is true for the chromium and tungsten analogs. This trend indicates that either the π-accepting ability of carbenes is moderately less than the silylenes or the σ-donating ability of carbenes is moderately greater than the silylene ligands. In reality, both of these proposals may be true to a degree that cannot be quantified with certainty. One can merely state that the electron donation to electron accepting ratio for the carbene is distinctly larger than the ratio for the silylenes.

These data are consistent with theoretical calculations that predict the σ-donor/π-acceptor ratio to be smaller for N-heterocyclic silylenes in comparison to the corresponding carbenes. Consequently, Boehme and Frenking anticipate the M→L bond strength to be weaker for N-heterocyclic silylenes in comparison to the corresponding carbenes [14].

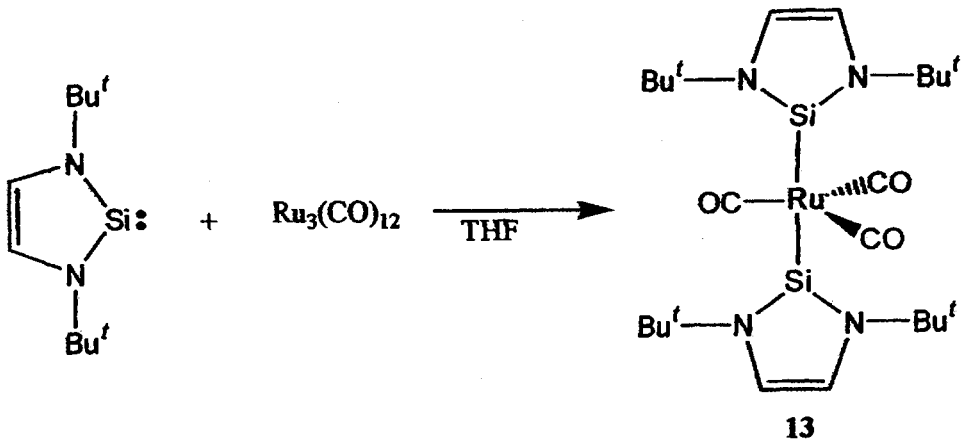

(3)

Table 2
Metal silicon bond lengths, cone angle and ^{29}Si-NMR values for metal silylene complexes

Compound	Compound number	^{29}Si (ppm)	Average M–Si (pm)	Estimated cone angle (°) of silylene
$Cr(\mathbf{1})_2(CO)_4$	**6**	136.9	232.9	110
$Cr(\mathbf{2})_2(CO)_4$	**7**	170.3	232.6	113
$Mo(\mathbf{1})_2(CO)_4$	**8**	119.3	247.1	106
$Mo(\mathbf{2})_2(CO)_4$	**9**	155.3	248.0	110
$W(\mathbf{1})_2(CO)_4$	**10**	97.8	247.1	106
$W(\mathbf{2})_2(CO)_4$	**11**	137.1	NA	NA
$Fe(\mathbf{1})(CO)_4$	**12**	111.6	219.6	119
$Ru(\mathbf{1})_2(CO)_3$	**13**	110.2	233.0	107, 113
$Ni(CO)_2(\mathbf{1})_2$		97.5	221.2	117, 110
$Ni(\mathbf{1})_3$		110.6	215.2	119
$Ni(\mathbf{2})_3$		144.6	215.8	119

Although it is difficult to determine quantitatively relative σ-donor and π-acidic effects between the stable silylenes, carbenes and phosphines, the data in Table 1 suggest that silylene **1** is roughly equivalent to PPh_3 in terms of its electronic behavior, with the order of σ-donator/π-acceptor ratios following the approximate trend: carbenes **4** and $\mathbf{5} > PR_3 > PPh_3 \sim \mathbf{1} > \mathbf{2} > P(OR)_3 > P(OAr)_3$. Though there is little difference in the chromium series in the frequencies for **1**, **2**, and triphenylphosphine, a trend becomes increasingly discernable as one proceeds down the triad to molybdenum and tungsten. While the CO frequencies for triphenylphosphine and **1** remain quite similar for these metals, the CO shift for **2** indicates a notably stronger CO bond. As **2** does not benefit from aromatic delocalization of electrons, this shift may be due to increased back-bonding to **2** in comparison to **1**, an effect which presumably becomes more pronounced down the triad.

Like the stable carbenes, the silylene ligands are much more inert to substitution than phosphines, a feature that may lend greater stability to their metal-complexes. In addition, the CO stretching frequencies also suggest that electronically, there is very little difference between the saturated and unsaturated silylene ligands.

Crystallographic structures indicate a decrease in M–Si bond lengths (Table 2) going across the table (with a notable exception for $Ni(\mathbf{1})_2(CO)_2$). The trend down the column is more complex with a large increase going from the first row to the second row but no notable difference between the second and third row, a trend which is consistent with the relative atomic radii of transition metals in the same group. Again, no significant differences in the M–Si bond lengths were found between the unsaturated and the saturated silylene.

An estimation of the ligand cone angles is important for considering the steric effects the stable silylenes may have on metal complexes [15]. Table 2 shows the cone angles of the metal silylene complexes determined from crystallographic measurements. The bulkiness of the silylenes as ligands has a controlling effect on the geometry of the metal silylene complexes especially in the first row series. The silylenes occupy the sterically least demanding sites in these complexes and also limit the degree of substitution.

Complexation of the silylene results in a significant downfield shift in the ^{29}Si-NMR. The deshielding is strong for first row metals and decreases down the row. The deshielding is also less in the case of $Ni(\mathbf{1})_2(CO)_2$, presumably due to the lengthening of the Ni–Si bond.

3. Experimental

All reactions and manipulations were conducted under an argon atmosphere using standard Schlenk techniques. The d^6-metal carbonyl precursors (Cr, Mo, W) were purchased (Strem) and sublimed in vacuo before use. The d^8-metal carbonyls (Fe and Ru) were purchased (Aldrich) and used without further purification. All of the reaction solvents were dried and distilled in an inert atmosphere. ^{1}H-NMR and ^{13}C-NMR were obtained on a Bruker 300 MHz spectrometer and ^{29}Si-NMR were obtained on a Varian 500 MHz instrument. Photolyses were accomplished at 254 nm in a Rayonet photochemical reactor. IR and Raman data for **6**–**11** are summarized in Table 3.

Table 3
Carbonyl stretching frequencies for various complexes

Compound	Compound number	Raman (cm^{-1})	IR (cm^{-1}, benzene)
$Cr(\mathbf{1})_2(CO)_4$	**6**	1996 A_{1g}, 1927 B_{1g}	1889 E_u
$Cr(\mathbf{2})_2(CO)_4$	**7**	1993 A_{1g}, 1922 B_{1g}	1888 E_u
$Mo(\mathbf{1})_2(CO)_4$	**8**	2016 A_{1g}, 1947 B_{1g}	1904 E_u
$Mo(\mathbf{2})_2(CO)_4$	**9**	2009 A_{1g}, 1937 B_{1g}	1919 E_u
$W(\mathbf{1})_2(CO)_4$	**10**	2014 A_{1g}, 1936 B_{1g}	1896 E_u
$W(\mathbf{2})_2(CO)_4$	**11**	2006 A_{1g}, 1930 B_{1g}	1911 E_u

3.1. Synthesis of $Cr(\mathbf{1})_2(CO)_4$, **6**

Into a quartz reaction vessel, freshly sublimed $Cr(CO)_6$ (0.580 g, 2.64 mmol), **1** (0.258 g, 1.31 mmol) and 40 ml of THF was added, producing a light yellow solution. The reaction mixture was photolyzed at 254 nm and at 10°C for 20 h, affording a clear, light brown solution. The solution was transferred to a Schlenk flask and the solvent was evaporated from the mixture under vacuum (0.1 Torr) yielding a light green solid. The solid was gently heated at 60°C under vacuum 2 h in order to sublime any unreacted starting materials. Yellow, prism-shaped crystals were obtained by dissolving the crude product in warm (50°C) toluene, followed by slow cooling of the solution. Yield by NMR: 82%. ^{1}H-NMR (C_6D_6) δ 6.62 (s, 4H), 1.57 (s, 36H). ^{13}C-NMR (C_6D_6) δ 218.30 (*C*O), 121.76 (=*C*H), 56.10 (*C*(CH_3)$_3$), 32.84 (C(*C*H_3)$_3$). ^{29}Si-NMR (C_6D_6) δ 136.94.

3.2. Synthesis of $Cr(\mathbf{2})_2(CO)_4$, **7**

Into a quartz reaction vessel, freshly sublimed $Cr(CO)_6$ (0.370 g, 1.68 mmol), **2** (1.00 g, 5.05 mmol, three equivalents) and 100 ml of THF was added. The reaction mixture was photolyzed at 254 nm and at 10°C for 20 h. The red solution was transferred to a Schlenk flask and the solvent was evaporated from the mixture under vacuum (0.1 Torr) leaving a red–brown residue. The solid was gently heated at 60°C for under vacuum 2 h in order to sublime any unreacted starting materials. The remaining product was rinsed with three 10 ml fractions of hexane to remove any tetrameric disilene impurities. The residue was dissolved in toluene and filtered. Recrystallization from toluene produced yellow crystals. Isolated yield = 0.24 g (26%). ^{1}H-NMR (C_6D_6) δ 2.90 (s, 4H), 1.46 (s, 36H). ^{13}C-NMR (C_6D_6) δ 192.92 (*C*O), 55.00 (*C*H_2), 31.91 (*C*(CH_3)$_3$), 47.42 (C(*C*H_3)$_3$). ^{29}Si-NMR (C_6D_6) δ 170.32.

3.3. Synthesis of $Mo(\mathbf{1})_2(CO)_4$, **8**

Into a quartz reaction vessel, freshly sublimed $Mo(CO)_6$ (0.672 g, 2.55 mmol), **1** (0.250 g, 1.27 mmol) and 30 ml of THF was added to give a clear, light yellow solution. The reaction mixture was photolyzed at 254 nm and at 10°C for 24 h, affording a clear, light brown solution. The THF was evaporated in vacuo leaving a light brown solid. The flask was heated at 65°C to remove any unreacted $Mo(CO)_6$ and silylene. The remaining solid was dissolved in toluene at 50°C. Upon slow cooling, yellow, plate-shaped crystals were obtained. Yield by NMR: 84%. ^{1}H-NMR (C_6D_6) δ 6.63 (s, 4H), 1.62 (s, 36H). ^{13}C-NMR (C_6D_6) δ 210.00 (*C*O), 120.73 (=*C*H), 55.95 (*C*(CH_3)$_3$), 33.62 (C(*C*H_3)$_3$). ^{29}Si-NMR (C_6D_6) δ 119.303.

3.4. Synthesis of $Mo(\mathbf{2})_2(CO)_4$, **9**

Into a quartz reaction vessel, $Mo(CO)_6$ (0.444 g, 1.68 mmol), **2** (1.00 g, 5.05 mmol, three equivalents) and 100 ml of THF was added. The reaction mixture was photolyzed at 254 nm and at 10°C for 20 h. The resulting red solution was transferred to a Schlenk flask and the solvent was evaporated from the mixture under vacuum (0.1 Torr) leaving a brown residue. The solid was gently heated at 60°C for under vacuum 2 h in order to sublime any unreacted starting materials. The remaining product was rinsed with three 10 ml fractions of hexane to remove any tetrameric disilene impurities. The residue was dissolved in toluene and filtered. Recrystallization from toluene produced yellow crystals. Isolated yield = 0.34 g (33%). ^{1}H-NMR (C_6D_6) δ 2.93 (s, 4H), 1.44 (s, 36H). ^{13}C-NMR (C_6D_6) δ 214.79 (*C*O), 54.36 (*C*H_2), 31.73 (*C*(CH_3)$_3$), 46.82 (C(*C*H_3)$_3$). ^{29}Si-NMR (C_6D_6) δ 155.30.

3.5. Synthesis of $W(\mathbf{1})_2(CO)_4$, **10**

Into a quartz reaction vessel, freshly sublimed $W(CO)_6$ (1.69 g, 5.09 mmol), **1** (0.500 g, 2.55 mmol) and 50 ml of THF was added, producing a clear, light yellow solution. The reaction mixture was photolyzed at 254 nm and at 10°C for 24 h, affording a clear, light brown solution. The THF was evaporated in vacuo leaving a light brown solid. The flask was heated at 65°C to remove any unreacted $Mo(CO)_6$ and silylene. The remaining solid was dissolved in toluene at 50°C. Upon slow cooling, yellow, prism-shaped crystals were obtained. Yield by NMR: 71%. ^{1}H-NMR (C_6D_6) δ 6.61 (s, 4H), 1.56 (s, 36H). ^{13}C-NMR (C_6D_6) δ 204.90 (*C*O), 120.53 (=*C*H), 55.86 (*C*(CH_3)$_3$), 33.42 (C(*C*H_3)$_3$). ^{29}Si-NMR (C_6D_6) δ 97.781.

3.6. Synthesis of $W(\mathbf{2})_2(CO)_4$, **11**

Into a quartz reaction vessel, $W(CO)_6$ (0.591 g, 1.68 mmol), **2** (1.00 g, 5.05 mmol, three equivalents) and 100 ml of THF was added. The reaction mixture was photolyzed at 254 nm and at 10°C for 20 h. The resulting red solution was transferred to a Schlenk flask and the solvent was evaporated from the mixture under vacuum (0.1 Torr) leaving a brown residue. The solid was gently heated at 60°C for under vacuum 2 h in order to sublime any unreacted starting materials. The remaining product was rinsed with three 10 ml fractions of hexane to remove any tetrameric disilene impurities. The residue was dissolved in toluene and filtered. Recrystallization from toluene produced yellow crystals. Yield: 0.42 g (36%). ^{1}H-NMR (C_6D_6) δ 2.91 (s, 4H), 1.46 (s, 36H). ^{13}C-NMR (C_6D_6) δ 206.50 (*C*O), 54.13 (*C*H_2), 31.37 (*C*(CH_3)$_3$), 46.85 (C(*C*H_3)$_3$). ^{29}Si-NMR (C_6D_6) δ 137.11

Table 4
Crystal structure parameters for compounds **6**–**10**, **12**, and **13**

	6	**7**	**8**	**9**	**10**	**12**	**13**
Empirical formula	$C_{24}H_{40}CrN_4O_4Si_2$	$C_{24}H_{44}CrN_4O_4Si_2$	$C_{24}H_{40}MoN_4O_4Si_2$	$C_{24}H_{44}MoN_4O_4Si_2$	$C_{24}H_{40}WN_4O_4Si_2$	$C_{14}H_{20}FeN_2O_4Si$	$C_{23}H_{40}N_4O_3RuSi_2$
Formula weight	556.78	560.81	600.72	604.75	688.63	364.26	577.84
Temperature (K)	133(2)	133(2)	133(2)	133(2)	133(2)	113(2)	133(2)
Crystal system	Orthorhombic	Orthorhombic	Orthorhombic	Triclinic	Monoclinic	Monoclinic	Triclinic
Space group	*Pbca*	*Pbca*	*Pbca*	$P\bar{1}$	$P2(1)/c$	$C2/c$	$P\bar{1}$
Unit cell dimensions							
a (Å)	11.4332(7)	11.6795(8)	11.454(3)	8.9283(13)	14.9860(11)	18.167(3)	9.8140(8)
b (Å)	14.9132(8)	14.8556(13)	14.938(4)	8.9669(12)	17.0773(15)	9.4546(18)	16.5578(13)
c (Å)	16.6378(8)	16.3202(15)	17.102(4)	10.0869(14)	11.4696(9)	12.0226(11)	18.5912(14)
α (°)	90	90	90	67.411(2)	90	90	101.539(2)
β (°)	90	90	90	79.329(2)	90.013	121.550(8)	99.659(2)
γ (°)	90	90	90	79.741(2)	90	90	104.680(2)
V (Å^3)	2838.7(3)	2831.7(4)	2926.1(13)	727.59(18)	2935.3(4)	1759.8(5)	2786.2(4)
Z	4	4	4	1	4	4	4
D_{calc} (Mg m^{-3})	1.303	1.315	1.364	1.380	1.558	1.375	1.378
Absorption coefficient (mm^{-1})	0.523	0.524	0.564	0.568	4.051	7.684	0.678
Crystal size (mm^3)	$0.53 \times 0.51 \times 0.33$	$0.24 \times 0.22 \times 0.16$	$0.33 \times 0.29 \times 0.20$	$0.24 \times 0.22 \times 0.04$	$0.44 \times 0.32 \times 0.32$	$0.50 \times 0.30 \times 0.20$	$0.40 \times 0.35 \times 0.30$
Theta range for data collection (°)	2.45–28.33	2.50–28.32	2.38–27.47	2.21–28.33	1.81–25.00	5.48–56.98	1.95–28.35
Reflections collected	13 162	13 134	17 047	9945	11 508	1579	36 808
Independent reflections	3331	3442	3262	3434	5061	1188	12 911
Final R indices [$I>2\sigma(I)$]	$R_1 = 0.0278$, $wR_2 = 0.0729$	$R_1 = 0.0319$, $wR_2 = 0.0852$	$R_1 = 0.0356$, $wR_2 = 0.1038$	$R_1 = 0.0290$, $wR_2 = 0.0727$	$R_1 = 0.0352$, $wR_2 = 0.1026$	$R_1 = 0.0367$, $wR_2 = 0.1002$	$R_1 = 0.0238$, $wR_2 = 0.0631$

3.7. Synthesis of $Fe(\mathbf{1})_1(CO)_4$, **12**

To a 250 ml Schlenk flask, 0.50 g (2.55 mmol, two equivalents) of silylene and a stir bar was added. Diiron nonacarbonyl (0.463, 1.27 mmol) was added, followed by 20 ml THF. The initially light orange solution grew darker in color over a period of 24 h to ultimately afford a red solution. ^{1}H-NMR indicated the formation of one major product. The THF was stripped from the reaction flask leaving a dark residue in the flask. The flask was heated to ca. 70°C under vacuum to remove, via sublimation, any unreacted starting materials. The remaining material was redissolved in toluene and the solution was cooled in a refrigerator for several days after which X-ray quality crystals became apparent. X-ray crystallography confirmed the 5 coordinate, trigonal-bipyramidal product containing one silylene ligands. ^{1}H-NMR (C_6D_6) δ 6.43 (s, 4H), 1.26 (s, 36H). ^{13}C-NMR (C_6D_6) δ 216.90 (*C*O), 120.68 (=*C*H), 67.84 (*C*(CH_3)$_3$), 32.94 (C(*C*H_3)$_3$). ^{29}Si-NMR (C_6D_6) δ 111.64.

3.8. Synthesis of $Ru(\mathbf{1})_2(CO)_3$, **13**

To a 250 ml Schlenk flask, 1.00 g (5.10 mmol, six equivalents) of silylene and a stir bar was added. Triruthenium dodecacarbonyl (0.540, 0.85 mmol) was added, followed by 40 ml THF. The initially light orange solution grew darker in color over a period of 3 h to ultimately afford a red solution. ^{1}H-NMR indicated the formation of one major product (and trace amounts of a minor product). The THF was stripped from the reaction flask leaving a dark red residue in the flask. The flask was heated to ca. 70°C under vacuum to remove any unreacted silylene. The red material was redissolved in toluene and the solution was cooled in a refrigerator for several days after which, large, orange crystals became apparent. X-ray crystallography confirmed the 5 coordinate product containing two silylene ligands. ^{1}H-NMR (C_6D_6) δ 6.64 (s, 4H), 1.55 (s, 36H). ^{13}C-NMR (C_6D_6) δ 213.50 (*C*O), 120.17 (=*C*H), 56.21 (*C*(CH_3)$_3$), 33.14 (C(*C*H_3)$_3$). ^{29}Si-NMR (C_6D_6) δ 110.16.

3.9. Crystal structure determination

Intensity data for compounds **6–10**, **12**, and **13** were collected using a Bruker SMART ccd area detector mounted on a Bruker Platform goniometer equipped with graphite-monochromated Mo–K_α radiation. All structures were determined at temperatures below 150 K. The structures of all compounds were solved by direct methods and refined by full-matrix least-squares on F^2 (SHELXTL, Version 5). Hydrogen atoms were initially determined by geometry and refined by a riding model. Non-hydrogen atoms were refined with anisotropic displacement parameters. Crystal structure parameters are listed in Table 4.

4. Conclusion

In conclusion, the present study supports the view that the stable silylenes are an important new class of ligands with electronic properties similar to triaryl phosphines. Furthermore, the electronic differences that exist in the isolated silylenes do not appear to have a significant effect on the M–Si bond length. It has been shown that the steric bulkiness of the silylenes is strongly dependent on the N-substituent (with a cone angle variation of ca. 25° just between neopentyl and *t*-Bu). With *t*-Bu as the substituent the cone angle is large enough to limit substitution and control the geometry of the complex, especially among the first row metals. The ability to fine tune the steric properties of the stable silylene as a ligand without affecting the electronic properties associated with it may aid the development of stable silylenes as ligands for transition metal catalysts. A detailed study of the catalytic properties of metal–silylene complexes is under way.

5. Supplementary material

Crystallographic data for the structures reported in this paper have been deposited with the Cambridge Crystallographic Data Centre, CCDC No. 157178 for compound **6**, No. 157175 for compound **7**, No. 157179 for compound **8**, No. 157177 for compound **9**, No. 157174 for compound **10**, No. 141350 for compound **12** and No. 157176 for compound **13**. Copies of this information may be obtained free of charge from The Director, CCDC, 12 Union Road, Cambridge CB2 1EZ, UK (Fax: +44-1223-336033; e-mail: deposit@ccdc.cam.ac.uk or www: http://www.ccdc.cam.ac.uk).

Acknowledgements

The authors thank Jeffrey Hirsch for determination of the Raman spectra, and the National Science Foundation and the Organosilicon Research Center Sponsors for financial support.

References

[1] For reviews, see (a) T.D. Tilley, in: S. Patai, Z. Rappoport (Eds.), The Chemistry of Organosilicon Compounds, Wiley, 1989, chap. 24. (b) P.D. Lickiss, Chem. Soc. Rev. (1992) 271. (c) K. H. Pannell, H, K, Sharma, Chem. Rev. (1995) 1351. (d) C. Zybill, Top. Curr. Chem. 160 (1991) 1.

[2] Fischer carbenes exhibit electrophilic behavior in contrast to Schrock carbenes, which are normally nucleophilic. See (a) E.O. Fischer, A. Massböl, Angew. Chem. Int. Ed. Engl. 3 (1964) 580. (b) K.H. Dotz, E.O. Fischer, P. Hoffmann, F.R. Kreissel, U. Schubert, K. Weiss, Transition Metal Carbene Complexes, Verlag Chemie, 1983.
[3] C. Zybill, G. Müller, Angew. Chem. Int. Ed. Engl. 26 (1987) 669.
[4] S.K. Grumbine, G.P. Mitchell, D.A. Straus, T.D. Tilley, A.L. Rheingold, Organometallics 17 (1998) 5607.
[5] See for example (a) D.A. Straus, S.D. Grumbine, T.D. Tilley, J. Am. Chem. Soc. 116 (1994) 7801. (b) S.K. Grumbine, T.D. Tilley, J. Am. Chem. Soc. 116 (1994) 5495.
[6] For a review on stable silylenes see M. Haaf, T.A. Schmedake, R. West, Acct. Chem. Res. 23 (2000) 704.
[7] M. Denk, R. Hayashi, R. West, Chem. Commun. (1994) 33.
[8] R. West, M. Denk, Pure Appl. Chem. 68 (1996) 785.
[9] B. Gehrhus, P.B. Hitchcock, M.F. Lappert, H. Maciejewski, Organometallics 17 (1998) 5599.
[10] T.A. Schmedake, M. Haaf, B.J. Paradise, D.R. Powell, R. West, Organometallics 19 (2000) 3263.
[11] W.A. Herrmann, C. Köcher, Angew. Chem. Int. Ed. Engl. 36 (1997) 2162.
[12] (a) T. Weskamp, V.P.W. Böhm, W.A. Herrmann, J. Organomet. Chem. 585 (1999) 348. (b) L. Ackermann, A. Fürstner, T. Weskamp, F.J. Kohl, W.A. Herrmann, Tetrahedron Lett. 40 (1999) 4787. (c) M.G. Gardiner, W.A. Herrmann, C.-P. Reisinger, J. Schwartz, M. Spiegler, J. Organomet. Chem. 572 (1999) 239. (d) T. Weskamp, F.J. Kohl, W.A. Herrmann, J. Organomet. Chem. 582 (1999) 362. (e) W.A. Herrmann, C.-P. Reiseinger, M. Spiegler, J. Organometal. Chem. 557 (1998) 93. (f) T. Weskamp, W.C. Schattenmann, M. Speigler, W.A. Herrmann, Angew. Chem. Int. Ed. Engl. 37 (1998) 2490.
[13] S.H.A. Petri, D. Eikenberg, B. Neumann, H.-G. Stammler, P. Jutzi, Organometallics 18 (1999) 2615.
[14] C. Boehme, G. Frenking, Organometallics 17 (1998) 5801.
[15] N-heterocyclic silylenes cannot be viewed as true "cones" due to their planar configuration, and may be better described as "fences". See (a) J. Huang, H. Schanz, E.D. Stevens, S.P. Nolan, Organometallics 18 (1999) 2370. (b) T.E. Muller, D.M.P. Mingos, Transition Metal Chem. 20 (1995) 533.
[16] Detailed IR studies of analogous carbene complexes can be found in (a) K. Öfele, M. Herberhold, Z. Naturforsch. 28 (1973) 306. (b) P.B. Hitchcock, M.F. Lappert, P.L. Pye, J. Chem. Soc. Dalton Trans. (1977) 2160. (c) M.F. Lappert, P.L. Pye, G.M. McLaughlin, J. Chem. Soc. Dalton Trans. (1984) 1307. (d) M.F. Lappert, P.L. Pye, J. Chem. Soc. Dalton Trans. (1977) 1283.
[17] D.T. Dixon, J.C. Kola, J.A.S. Howell, J. Chem. Soc. Dalton Trans. (1984) 1307.
[18] F.A. Cotton, Inorg. Chem. 3 (1964) 702.
[19] R. Poiblank, M. Bigorgne, Bull. Soc. Chim. Fr. (1962) 1301.
[20] G.L. Hillhouse, B.L. Haymore, Inorg. Chem. 26 (1987) 1876.